The Proton/Electron Coupling Ratio at Heme *a* and Cu_A in Bovine Heart Cytochrome *c* Oxidase

Nazzareno Capitanio, Giuseppe Capitanio, Domenico Boffoli, and Sergio Papa*

Department of Medical Biochemistry and Biology, University of Bari, Piazza G. Cesare, 70124 Bari, Italy

Received August 15, 2000

ABSTRACT: Measurements of the H^+/heme *a*, Cu_A ratios for proton−electron coupling at these centers (redox Bohr effect) in CO-inhibited cytochrome *c* oxidase purified from bovine heart mitochondria, both in the soluble state and reconstituted in liposomes, are presented. In the soluble oxidase, the H^+/heme *a*, Cu_A ratios were experimentally determined upon oxidation by ferricyanide of these centers as well as upon their reduction by hexammineruthenium(II). These measurements showed that in order to obtain H^+/heme *a*, Cu_A ratios approaching 1, one-step full oxidation of both metal centers by ferricyanide had to be induced by a stoicheiometric amount of the oxidant. Partial stepwise oxidation or reduction of heme *a* and Cu_A did produce H^+/heme *a*, Cu_A ratios significantly lower or higher than 1, respectively. The experimental H^+/heme *a*, Cu_A ratios measured upon stepwise reduction/oxidation of the metals were reproduced by mathematical simulation based on the coupling of oxido−reduction of both heme *a* and Cu_A to p*K* shifts of common acid−base groups. The vectorial nature of the proton−electron coupling at heme *a*/Cu_A was analyzed by measuring pH changes in the external bulk phase associated with oxido−reduction of these redox centers in the CO-inhibited oxidase reconstituted in liposomes. The results show that the proton release associated with the oxidation of heme *a* and Cu_A takes place in the external aqueous phase. Protons taken up by the oxidase upon rereduction of the centers derive, on the other hand, from the inner space. These results provide evidence supporting the view that cooperative proton−electron coupling at heme *a*/Cu_A is involved in the proton pump of the oxidase.

Cytochrome *c* oxidase (COX) catalyzes the reduction of O_2 to H_2O by ferrocytochrome *c* and conserves the free energy made available as a membrane electrochemical proton gradient (PMF) (*1*−*3*). Electrons delivered by ferrocytochrome *c* to the low potential Cu_A and heme *a* pass from these to the binuclear heme a_3−Cu_B center, where O_2 is ultimately reduced to H_2O (*3, 4*). PMF generation results from consumption of protons from the inner (N) aqueous phase in the reduction of O_2 to H_2O by cytochrome *c*, located at the outer (P) side of the membrane (*1*−*3*), and from net proton pumping from the N to P phase (*3*). From time to time, it has been proposed that proton pumping in COX is directly coupled to oxido−reduction of Cu_A (*5, 6*), heme *a* (*7*−*11*), and the binuclear center (*12, 13*). Possible candidates for such a role are, in principle, those metal centers which exhibit intrinsic coupling of electron transfer with proton transfer (*2, 14*). This linkage, which has been denominated redox Bohr effect (*2, 15*) by analogy with the cooperative linkage phenomena in hemoglobin (*16*), results in pH dependence of the midpoint redox potential (*14, 17*) and in net proton release/uptake by the enzyme associated with oxidation/reduction of the metals, respectively (*18*).

Our group is carrying out a systematic analysis of the H^+ release/uptake (H^+/COX) associated with oxidation/reduction of the metal centers in cytochrome *c* oxidase isolated from bovine heart mitochondria in both the unliganded and CN-liganded or CO-liganded oxidase (*19*−*21*). In the CO-liganded enzyme both heme a_3 and Cu_B are clamped in the reduced state, and electron/proton coupling at heme *a* and Cu_A can be analyzed in the absence of interaction with Cu_B and heme a_3 (*22*). Under these conditions we obtained H^+/COX ratios which varied between 0.60 and 0.90 in the pH range 6.0−8.6 (*19*). This redox-coupled H^+ transfer was initially attributed to heme *a*, as the available data indicated the E′m of Cu_A to be pH independent (*23*; but see *24*, *25*). Electron/proton coupling at heme *a* only with H^+/COX ratios of 0.6−0.9 (*19*) would, however, be in apparent conflict with previous measurements of the pH dependence of the Em of heme *a*, which in the CO-inhibited COX is reported to amount to not more than −20 mV per pH unit increase in the 6−8 pH range (*22, 26*). Prompted by this consideration, Verkovsky et al. (*27*) measured proton release coupled to oxidation of heme *a* and Cu_A in CO-inhibited COX and reported H^+/COX ratios varying between 0.43 and 0.20, only in the pH range 6.6−7.7.

In a recent work (*21*), we refined the analysis of the H^+/heme *a*, Cu_A ratio in the CO-inhibited COX, with direct measurement of the balance between the oxidizing equivalents added as ferricyanide to the CO-inhibited fully reduced COX, the equivalents of heme *a*, Cu_A oxidized, and the H^+ released upon oxidation, all taken back up by the oxidase upon rereduction of the metal centers. The results definitely confirmed H^+/heme *a*, Cu_A ratios varying between 0.65 and 0.90 in the pH range 6.0−8.5. The pH dependence of the H^+/heme *a*, Cu_A ratios could be best-fitted by a function

* To whom correspondence should be addressed. Telephone: +39 (080) 5478428. Fax: +39 (080) 5478429. E-mail: papabchm@cimedoc.uniba.it.

10.1021/bi001940z CCC: $19.00 © 2000 American Chemical Society
Published on Web 11/17/2000

involving two redox-linked acid−base groups, at least, with pK_o and pK_r values of 5.4−6.9 and 7.3−9.0, respectively. Redox titrations in the same samples of the CO-inhibited oxidase showed that Cu_A and heme *a* exhibited superimposed E′m values which decreased, for both metals, by around 20 mV/pH unit increase in the range 6.0−8.5. A model in which oxido−reduction of heme *a* and Cu_A are both linked to the p*K* shifts of two acid−base groups provided a satisfactory fit for the pH dependence of the E′m of heme *a* and Cu_A (*21*).

In this paper, measurements of the H^+/heme *a*, Cu_A ratios for proton−electron coupling at these centers (redox Bohr effects) in CO-inhibited cytochrome *c* oxidase purified from bovine heart mitochondria, both in the soluble state and in the oxidase reconstituted in liposomes, are presented. For the measurements of the soluble oxidase, both the experimental conditions previously used by our groups (*21*) and those of Verkovsky et al. (*27*) were applied. The results on the soluble oxidase show that in order to obtain H^+/heme *a*, Cu_A ratios approaching 1, one-step full oxidation of both metal centers has to be induced by addition of a stoicheiometric amount of ferricyanide (see *19*, *21*). Partial oxidation or reduction of heme *a* and Cu_A does produce H^+/heme *a*, Cu_A ratios significantly lower (see also *27*) or higher than 1, respectively. These observations solved the apparent discrepancy of the results of Verkovsky et al. (*27*) with ours (*19*−*21*) and provide additional, independent evidence of coupling of both heme *a* and Cu_A to common acid−base group(s).

The experiments with the CO-inhibited oxidase reconstituted in liposomes showed that proton translocation associated with oxido−reduction of heme *a*, Cu_A is vectorial. Protons were released in the bulk external phase upon oxidation of heme *a*, Cu_A and taken up from the inner space upon reduction of these centers.

MATERIALS AND METHODS

Materials. Horse heart cytochrome *c* (type VI), antimycin A, and myxothiazol were from Sigma Chemical Co.; hexammineruthenium(II) chloride was from Aldrich; potassium ferricyanide was from BDH Chemicals Ltd. All other reagents were of the highest purity grade commercially available.

Enzyme Preparation and Reconstitution in Liposomes. Cytochrome *c* oxidase was purified from beef heart mitochondria as described in ref *28*. The nanomoles of (heme *a* + a_3)/mg protein was about 10, and SDS-PAGE analysis revealed the complete set of 13 subunits (*29*). The activity of the enzyme preparations, measured polarographically, was around 300 TN/s. Reconstitution of cytochrome *c* oxidase in phospholipid vesicles was performed by the cholate dialysis method as described in ref *30*, with the following differences: (i) the aa_3/phospholipid ratio was doubled (final concentration of cytochrome *c* oxidase was 6 μM); (ii) in the last dialysis medium 1 mM K−Hepes was omitted. These changes did not affect the respiratory control ratio, which was even higher than in the "standard" procedure (never below 15, when measured polarographically (*31*) or the right-side-out orientation of the oxidase molecule in the liposomal membrane (never below 80% (*32*)).

Measurements of pH and Redox Changes. Simultaneous recordings of absorbance and pH changes were carried out with a diode-array spectrophotometer and a combined electrode, respectively, with accuracy of 5×10^{-4} absorbance and 10^{-3} pH unit (overall response time <1 s). The diode-array spectrophotometer was used in the multiwavelength mode, and simultaneous recording of pH and difference absorbance changes was carried out. The wavelengths selected, 550−630, 590−630, 605−630, and 800−710 nm, were used to determine cytochrome *c*, heme a_3−CO, heme *a*, and Cu_A, respectively. The mutual optical overlapping among cytochrome *c*, heme a_3−CO, and heme *a* was removed solving the following matrix:

$$A_{550-630} = [\text{cyt } c](19.1) + [\text{heme } a_3\text{−CO}](3.81) + [\text{heme } a](-0.25)$$

$$A_{590-630} = [\text{cyt } c](-1.11) + [\text{heme } a_3\text{−CO}](9.75) + [\text{heme } a](6.03)$$

$$A_{605-630} = [\text{cyt } c](-0.36) + [\text{heme } a_3\text{−CO}](2.85) + [\text{heme } a](21.73)$$

The differential extinction coefficients are from ref *33*; the absorbance change at 800−710 nm was corrected for the contribution of cytochrome *c* ($\Delta\epsilon = 0.36$ mM^{-1}), and a $\Delta\epsilon = -1.0$ mM^{-1} was used for Cu_A (*34*). Ferricyanide was assayed at 420−500 nm using a $\Delta\epsilon$ of 1.0 mM^{-1}.

Mathematical Procedure To Simulate Proton Release−*Uptake upon Stepwise Oxido*−*Reduction of CO-Liganded Cytochrome c Oxidase*. Considering a given number of fully reduced CO-liganded oxidase molecules and different amounts of added oxidizing equivalents, the number of all the possible oxidized species can be predicted adapting the general eq 1, used to calculate the simple combination of *n* objects of *k* class:

$$C_{n,k} = n!/(k!(n-k)!) \quad (1)$$

where *n* is the number of redox active metal centers (2 times the amount of cytochrome oxidase, since only Cu_A and heme *a* can be oxidized per each molecule of the CO-liganded enzyme); *k* is the amount of oxidizing equivalents added (as ferricyanide). Each molecule of the enzyme can be present with both redox centers oxidized, both reduced, or one reduced and the other oxidized. Since it is unlikely that heme *a* can be oxidized before Cu_A in the same molecule, only the class in which both redox centers are oxidized in one or more oxidase molecules (with or without Cu_A oxidized in one or more of the remaining molecules) and that in which Cu_A is oxidized in one or more molecules are considered physically possible among all the combination classes.

Coupling of oxido−reduction of both heme *a* and Cu_A to common acid−base group(s) (*21*) brings with itself the assumption that release of nH$^+$ takes place *only* when both Cu_A and heme *a* are oxidized in the same COX molecule. It can also be assumed that in those COX molecules in which only Cu_A is oxidized, rapid electronic redistribution with heme *a* occurs resulting in 50% oxidation of Cu_A and heme *a*, which is isopotential with Cu_A (*21*). The H^+/heme *a*, Cu_A ratio, expected upon additions of oxidizing equivalents to different samples of CO−COX, can be calculated by

$$H^+/\text{heme } a,\ Cu_A = nN_a/(N_a + 0.5N_b) \quad (2)$$

where N_a is the number of oxidase with both Cu_A and heme *a* oxidized and N_b is the number of oxidase molecules where only Cu_A is oxidized.

The same rationale can be used to simulate the proton uptake following the addition of different amounts of reducing equivalents to the mixed valence CO-liganded enzyme. In this case uptake of nH^+ will take place just upon reduction of heme *a* or Cu_A(1 electron equivalent/COX) in a given mixed valence CO-liganded oxidase molecule; as a consequence, further reduction of the second metal (2 electron equivalents/COX) will not result in further H^+. In this case the H^+/heme *a*, Cu_A coupling number will be given by

$$H^+/\text{heme } a,\ Cu_A = (nN_a + nN_b)/(N_a + 0.5N_b) \quad (3)$$

where N_a is the number of oxidase molecules with both Cu_A and heme *a* reduced and N_b is the number of the oxidase molecules with reduction of only one of the two centers.

In addition to the above treatments, which relate to the *initial* statistical distribution of all the possible combinatory classes of the oxidase molecules, the situation was also dealt with in which all the molecules of the CO-liganded oxidase generated upon addition of the oxidant or the reductant reached the same Nernst redox equilibrium through intermolecular cytochrome *c*-mediated electron transfer.

RESULTS

Measurements of the H^+/heme a, Cu_A Ratios in the Soluble Cytochrome c Oxidase (COX). Figure 1 shows the time course of oxidation of heme *a*, in CO-inhibited reduced COX, upon addition of an amount of ferricyanide equivalent to 95% of the sum of Cu_A, heme *a*, and added cytochrome *c*. These centers were previously fully reduced by succinate by means of a trace of broken mitochondria, followed by the addition of myxothiazol plus antimycin A, which completely blocked any further delivery of electrons from succinate. Ferricyanide gave, under these conditions, permanent oxidation of heme *a* as well as of Cu_A and added cytochrome *c* (see also Table 1). Oxidation of the metal centers was accompanied by a rapid release of 0.72 H^+/heme *a*, Cu_A after which there was no further pH change. Measurement of the stoicheiometry balance of the reaction showed that the sum of the oxidation extents of cytochrome *c*, Cu_A, and heme *a* corresponded exactly to the oxidizing equivalents of ferricyanide added (Table 1). These measurements thus excluded any contribution to proton release of spurious acidification reaction, like oxidation of ubiquinol, in the trace of broken mitochondria as suggested by Verkovsky et al. (*27*) or oxidation of CO to HCO_3^- by ferricyanide. The traces in Figure 1 show that the H^+ release associated with oxidation of Cu_A and heme *a* was reversed upon stepwise rereduction of the metal centers by successive additions of substoicheiometric amounts of hexammineruthenium(II). It can, however, be noted that the first addition of hexammineruthenium, producing only 19% reduction of heme *a* (and Cu_A), resulted in proton uptake giving an H^+/heme *a*, Cu_A ratio of 1.2 (see also Figure 2). Successive additions of hexammineruthenium(II), producing further reduction of the two metal centers, resulted in proton uptake with progressively decreasing H^+/heme *a*, Cu_A ratios (see also Figure 2). Once heme *a* and Cu_A were fully rereduced by hexammineruthenium(II) (it should be noted

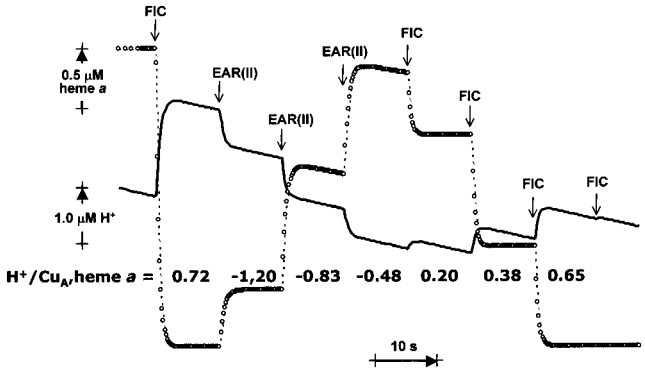

FIGURE 1: Measurements of scalar H^+ transfer associated with consecutive stepwise reduction−oxidation of CO-liganded cytochrome *c* oxidase. A total of 2.5 μM of purified bovine cytochrome *c* oxidase was suspended in 0.15 M KCl, 0.1 mM EDTA and supplemented with 1.0 μM cytochrome *c*, 0.2 mg/mL frozen−thawed, broken beef heart mitochondria, and 0.5 μg of rotenone/mL (pH 7.2). The suspension was bubbled first with nitrogen and then with pure CO. A combined pH electrode was inserted in the cuvette containing the CO-saturated suspension, and this was then layered with deaerated mineral oil. Addition of 5 mM succinate to the CO saturated COX caused formation of the fully reduced CO-liganded cytochrome *c* oxidase in 10−15 min (*21*). The solid trace shows pH changes, calibrated with titrated HCl solutions; the dotted curve shows the results of spectral deconvolution of redox changes of heme *a* after removal of the mutual optical overlapping of cytochrome *c* and heme a_3−CO (see Materials and Methods and ref *21*). The fully reduced CO-liganded enzyme was supplemented with 0.1 μM antymicin A plus 0.3 μM myxothiazol and pulsed with 6.0 μM ferricyanide. The mixed valence CO-liganded aa_3, so generated, was first rereduced and then reoxidized by consecutive additions of hexammineruthenium(II) and ferricyanide (substoicheiometric with respect to sum of the equivalents of cyt *c* + Cu_A + heme *a*), respectively.

that in these oxido−reduction titrations, heme *a* and Cu_A were always oxidized/reduced to the same extent), their oxidation was initiated again by successive additions of substoicheiometric amounts of ferricyanide. The first addition of ferricyanide, giving 21% oxidation of heme *a* (and Cu_A), resulted in an H^+/heme *a*, Cu_A ratio of only 0.20. Successive additions of ferricyanide, giving further oxidation of the metal centers, resulted in proton release with H^+/heme *a*, Cu_A ratios which progressively increased, until a value of 0.65 was reached upon the last addition of ferricyanide, which completed the oxidation of the redox centers of CO-inhibited COX (see also Figure 2). A similar pattern of decreasing H^+/heme *a*, Cu_A ratios, from values above to below 1 for proton uptake, upon progressive reduction of the metal centers, and of increasing H^+/heme *a*, Cu_A ratios for proton release, upon progressive reoxidation of the metal centers, were experimentally obtained when increasing amounts of hexammineruthenium (II) and ferricyanide were respectively added to separate samples of CO-inhibited COX (not shown).

Evidence has been provided (*21*) showing that oxido−reduction of both heme *a* and Cu_A is linked to p*K* shifts of two acid−base groups, at least, in CO-inhibited COX. A consequence of this interactive H^+/e^- cooperative coupling is that reduction of either heme *a* or Cu_A in one molecule in a population of CO-inhibited COX is enough to cause maximal protonation, at the given pH, of the two acid−base group(s) (Figure 7). Reduction of the second metal center in the same COX molecule will not cause any further H^+ uptake. Release of the H^+ bound to the reduced COX molecule will take place only when both Cu_A and heme *a* in

Table 1: Analysis of Ferricyanide-Induced Redox Transitions of the Metal Centers in the CO-Liganded Reduced Cytochrome *c* Oxidase and Associated H^+ Release[a]

1 ferriCN added	2 cyt *c* oxidized	3 heme *a* oxidized	4 Cu_A oxidized	2 + 3 + 4	1/(2 + 3 + 4)	a_3−CO	a_3−CO + FerriCN	H^+_R/heme *a*, Cu_A
6.00	1.02	2.54	2.50	6.06	0.99	2.98	2.95	0.72

[a] The experimental conditions are those described in the legend of Figure 1. The values indicate μM concentrations of cytochrome *c*, heme *a*, and Cu_A that are oxidized upon addition of ferricyanide; a_3−CO and a_3−CO + ferriCN indicate the concentrations of the a_3^{2+}−CO compound, before and after the addition of ferricyanide, respectively; H^+_R is proton release associated with oxidation of the heme *a* and Cu_A. The concentrations of COX and cytochrome *c* were 2.5 and 1 μM, respectively.

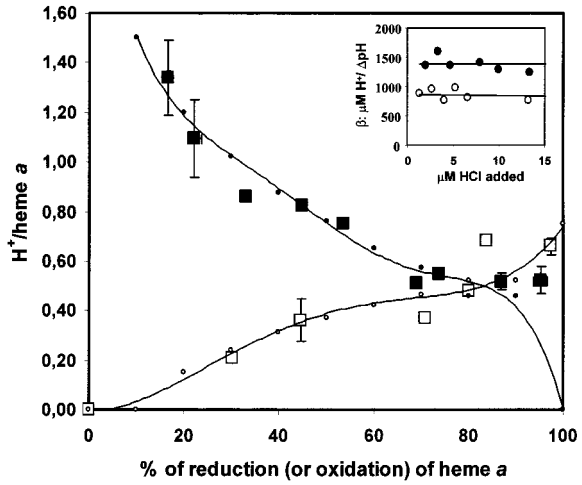

FIGURE 2: H^+ release associated with stepwise reductive−oxidative titration of Cu_A and heme *a* in CO-liganded cytochrome *c* oxidase. The experimental conditions are those described in the legend to Figure 1. The measured H^+/heme *a*, Cu_A ratios for proton uptake−release associated with consecutive stepwise reductive−oxidative titrations with hexammineruthenium(II) and ferricyanide are shown by black and white squares, respectively. Simulation of the H^+/heme *a*, Cu_A ratios is shown by small black circles for reductive titration and small white circles for oxidative titration. The bars on the symbols (where given) indicate the standard errors of the mean value of three to four measurements. The inset shows measurements of the buffering capacity (β) of 10 μM cytochrome *c* oxidase suspended in the reaction medium in the absence (white circles) and in the presence (black circles) of 10 μM cytochrome *c* plus 0.4 mg mitochondria/mL. It can be noted that the buffering power remained constant upon titration with increasing amounts of added HCl. For other details concerning the mathematical procedure and the equations used for the simulation, see Materials and Methods.

the same COX molecule are oxidized (Figure 7). Consequently the initial H^+/heme *a*, Cu_A ratios for proton uptake and release upon reduction and oxidation of the CO-inhibited COX population, respectively, will vary, under these conditions, with the extent of reduction and oxidation of these centers attained during the redox titration. The simulation curves for the H^+/heme *a*, Cu_A ratios that can be calculated by applying the probability eqs 2 and 3 (see Materials and Methods) for progressive oxidation and reduction of COX molecules, respectively, are presented in Figure 2. The simulation curves show how the calculated H^+/heme *a*, Cu_A ratios decrease with increasing extents of reduction of the metal centers and increase with increasing extents of oxidation of the metal centers in CO−COX. The experimentally determined H^+/heme *a* (or H^+/Cu_A) ratios practically coincided with those obtained from these simulation curves. It can also be noted that the H^+/heme *a*, Cu_A ratios, measured or simulated in the present work for partial 30−70% oxidation of heme *a* (and Cu_A) in the CO-inhibited pre-reduced COX, are essentially the same as those reported, under these conditions, by Verkovsky et al. (*27*). The present observations show that, under the prevailing conditions of the redox titrations, low and high H^+/heme *a*, Cu_A ratios can be obtained depending on the oxidation−reduction state of the COX molecules and provide additional independent evidence for the occurrence of interacting coupling of two (or more) acid−base groups with oxido−reduction of both heme *a* and CuA.

It can be noted that the experimental and simulated (continuous curves in Figure 2) H^+/heme *a*, Cu_A ratios for proton release and uptake associated with oxidation and reduction of these centers, respectively, refer to the initial proton translocation obtained upon addition of the oxidant or of the reductant when different oxido−reduction classes of the oxidase are generated. The initial different oxido−reduction classes of the oxidase will, however, reach with time the same Nernst redox equilibrium through intermolecular cytochrome *c*-mediated electron transfer. It can be predicted on the basis of the model presented in Figure 7, and eqs 2 and 3, that cytochrome *c*-mediated intermolecular electron redistribution between oxidase molecules having both heme *a* and Cu_A reduced with those with both centers oxidized will cause, up to an overall oxidation extent of 50% of heme *a* and Cu_A, reuptake of the protons initially released upon the addition of the oxidant. This intermolecular electron redistribution among the different classes of oxidase molecules, whose only detectable sign is given by the reuptake of the protons initially released, was, however, found to be extremely slow (Figure 3). With a $t_{1/2}$ of around 3 min, it did not affect significantly the initial H^+ release associated with oxidation of heme *a* and Cu_A, which has a $t_{1/2}$ of less than 1 s. The same conclusion can be reached from the simulation (not shown) of the situation arising when intermolecular Nernst equilibrium is reached (see also the model in Figure 7). This simulation shows, in fact, that in the stepwise oxidative titration, at equilibrium, the partial H^+/heme *a* (or H^+/Cu_A) ratios for proton release will be zero till 50% oxidation of heme *a* (and Cu_A) is reached. Then any further oxidation step will produce maximal H^+/heme *a* (or H^+/Cu_A) ratios of 0.75. Conversely, in the stepwise reductive titration, at equilibrium, the H^+/heme *a* (or H^+/Cu_A) ratios for proton uptake will be constantly 1.5 till 50% reduction of heme *a* (and Cu_A) is reached. Any further reduction step will result in H^+/heme *a* (or H^+/Cu_A) ratios of zero. This pattern is thus inconsistent with the H^+/heme *a*, Cu_A ratios experimentally obtained which, on the other hand, fit perfectly the simulation curves obtained on the basis of the initial generation of different oxido−reduction classes of the oxidase molecules (eqs 2 and 3) (Figure 2).

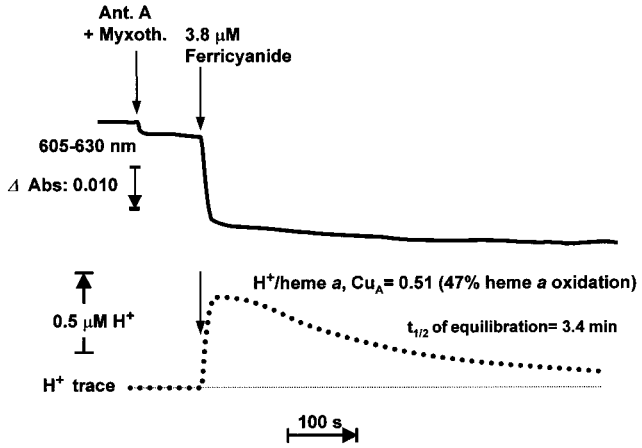

FIGURE 3: Measurement of scalar H^+ transfer associated with partial oxidation of reduced CO-liganded cytochrome *c* oxidase. The experimental conditions are those described in the legend of Figure 1. The amount of ferricyanide added was chosen in order to cause around 50% oxidation of heme *a* (and Cu_A, not shown). The time course of the pH change was reconstructed from the original trace point by point at interval times of 5 s and corrected for a constant baseline drift; note the much larger time scale with respect to that of Figure 1.

Measurements of H^+/heme a, CuA Ratios in Liposome Reconstituted Cytochrome c Oxidase. The vectorial nature of the proton−electron coupling at heme *a*, Cu_A was analyzed by following pH changes in the external bulk phase associated with oxido−reduction of the centers in the CO-liganded oxidase reconstituted in liposomes (COV). The oxidase was brought into the reduced CO-inhibited state by succinate oxidation, mediated by a trace of broken mitochondria and cytochrome *c*. The spectrophotometric and potentiometric traces presented in Figure 4 show that the oxidation of heme *a* (Cu_A and cytochrome *c* not shown) induced by the addition of an amount of ferricyanide equivalent to the sum of the cytochrome *c*, heme *a*, and Cu_A was accompanied by a rapid H^+ release, which continued, as expected, during the rereduction of the metal centers by succinate oxidation. The rapid acidification phase could be better separated from the latter in the experiments depicted in Figure 4 parts b and c in which the succinate oxidation was slowed by the addition of malonate. Practically the same rapid acidification, but suppression of the second slow acidification phase, was observed before when adding ferricyanide myxothiazol *plus* antimycin A, which blocked further succinate oxidation (Figure 4d). Mathematical resolution of the proton translocation phases (Figure 5) showed that the slow acidification reaction, which followed the initial rapid acidification associated with oxidation of heme *a* and Cu_A, exhibited the same kinetic constant as that for the rereduction of heme *a* (and Cu_A). The overall acidification process, after having reached a maximum upon completion of the rereduction of the metal centers, showed a slow and small reversal, evidently due to pH equilibration between the outer and inner space of COV.

In Figure 6 the H^+ release/ferricyanide ratios measured in a series of experiments as those presented in Figure 4, in which the rate of succinate oxidation was progressively inhibited by increasing amount of malonate, are presented. The overall reduction of added ferricyanide by succinate should have resulted in the 1:1 stoichiometric H^+ release in the external medium. An extra acidification was, however,

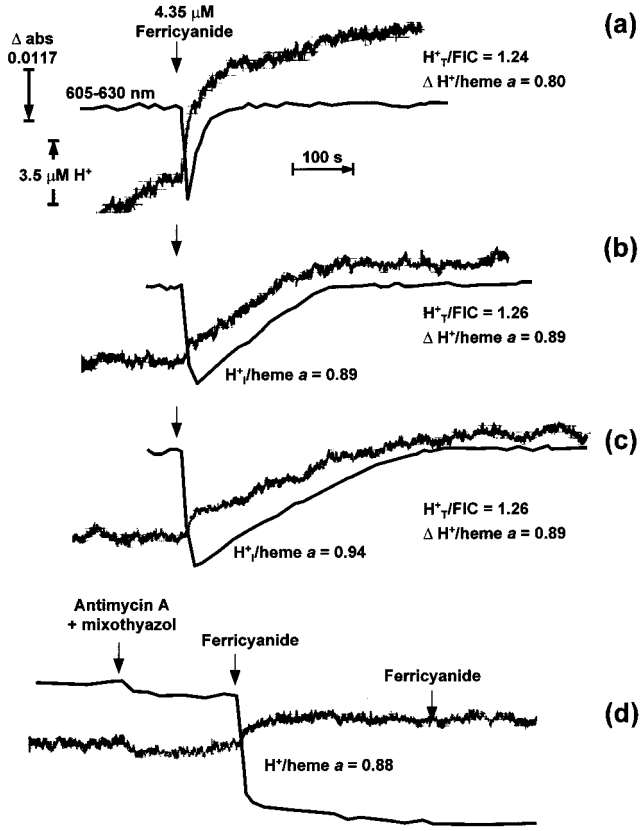

FIGURE 4: Analysis of the sidedness of the H^+ transfer associated with redox transitions of metal centers in the CO-liganded cytochrome *c* oxidase vesicles. A concentration of 1.5 μM COV was suspended in 0.15 M KCl and supplemented with 1.5 μM cytochrome *c*, 1 μg/mL valinomycin, and 0.1 mg/mL frozen−thawed beef heart mitocondria, pH 7.4. The suspension was gently bubbled first with nitrogen and then with CO for 2 min and then covered with a layer of mineral oil to prevent further gas exchange. Addition of 3 mM succinate produced anaerobiosis and full reduction of cytochrome *c* oxidase in 10−15 min. Where indicated, anaerobic 4.35 μM ferricyanide was added and heme *a* absorbance and pH changes monitored simoultaneously as described in Materials and Methods and in the legend to Figure 1: (a) no malonate present; (b) and (c) in the presence of 1.0 and 1.5 mM malonate, respectively. In (d) the addition of ferricyanide was preceded by the addition of 0.1 μM antimycin A plus 0.3 μM myxothiazol. H^+_T/FIC indicates the ratios between the total amount of H^+ released following the oxidation/reduction cycle and the amount of oxidizing equivalents added as ferricyanide; H^+_I/heme *a* indicates the ratios between the initial proton release associated with the rapid oxidation of metal centers elicited upon addition of ferricyanide and the amount of oxidized heme *a*; ΔH^+/heme *a* indicates the ratios between the extra H^+ release with respect to the amount of ferricyanide added and the amount of heme *a* undergoing oxido−reduction.

observed at all the malonate concentrations, which exceeded the amount of ferricyanide added, the ratio H^+ release/ferricyanide added amounting to 1.20−1.25. This extra acidification, referred to the extent of heme *a* (and Cu_A) oxidized, gave an H^+/oxidase ratio of 0.75−0.85. The same H^+/heme *a*, Cu_A ratio of around 0.80 could be calculated from the initial rapid acidification associated with the oxidation of heme *a* and Cu_A. These results thus show that the transient oxidation of heme *a* (and Cu_A) results in rapid H^+ release in the outer bulk phase; i.e., the Bohr protons associated with the oxidation of heme *a* and Cu_A are released from the oxidase in the external aqueous space. If the redox Bohr protons released in the external phase were then taken

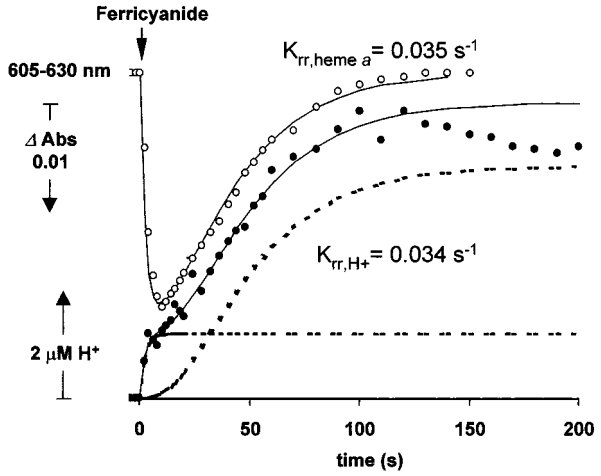

FIGURE 5: Mathematical deconvolution of proton transfer associated with oxidation/rereduction of heme *a* in CO-liganded cytochrome *c* oxidase vesicles. The experimental conditions are those described in the legend of Figure 4. Mathematical treatment was applied, as an example, to the traces shown in Figure 4b. The time courses for the oxidation/rereduction cycle of heme *a* and the associated proton release were fitted in both cases with equations resulting from the sum of two exponentials as follows: $\Delta Abs_{605-630nm} = A((1 - \exp(-k_{ox}t)) - (1 - \exp(-k_{rr}t))^n)$, $H^+ = B(1 - \exp(-k_{ox}t)) + C(1 - \exp(-k_{rr}t))^n$, where *A* represents the final absorbance level of heme *a* in the rapid initial oxidation phase, *B* is the final H^+ release associated with the rapid initial oxidation phase, *C* is the final H^+ release associated with the slow rereduction phase, k_{ox} and k_{rr} are the exponential constants for the rapid oxidation and slower rereduction phases, respectively, and *n* is an exponential introduced to improve the fitting of the traces because of the presence of a lag in the slow phase. The white and black circles are the extents of the absorbance and pH changes taken at different interval times, respectively. Continuous lines are the best fits of the experimental points; for the fitting of the pH trace, all the points collected after the completion of the rereduction of heme *a* were omitted; dashed lines show the resolution of the overall pH fit into the two phases of pH changes.

up by the oxidase from the same space upon rereduction of heme *a* and Cu_A by succinate, no net excess of H^+ release, with respect to the ferricyanide added, should have been left when heme *a* and Cu_A were fully rereduced. Reuptake of the Bohr protons did, instead, occur with a considerable delay after rereduction of the redox centers (see Figure 5). These observations show that the Bohr protons associated with rereduction of heme *a* and Cu_A are taken up from the inner aqueous space. This was confirmed by the observation that in the presence of CCCP, which equilibrates the inner and outer pH changes, the same initial rapid acidification was observed upon oxidation of heme *a* by ferricyanide, as in the coupled system, but at the completion of the rereduction of heme *a* no extra-acidification, with respect to the ferricyanide added, was observed (Figure 6B).

DISCUSSION

The results presented in this paper provide additional, independent evidence of cooperative coupling in cytochrome *c* oxidase of the redox state of both heme *a* and Cu_A with the protonation state of common acid−base groups. The interaction of both heme *a* and Cu_A with two (or more) common acid−base groups results, under the equilibrium conditions of the redox titration, in a pH dependence of the Em of both redox centers smaller than −29 mV/pH unit increase (*21*). It can incidentally be noted that redox titrations

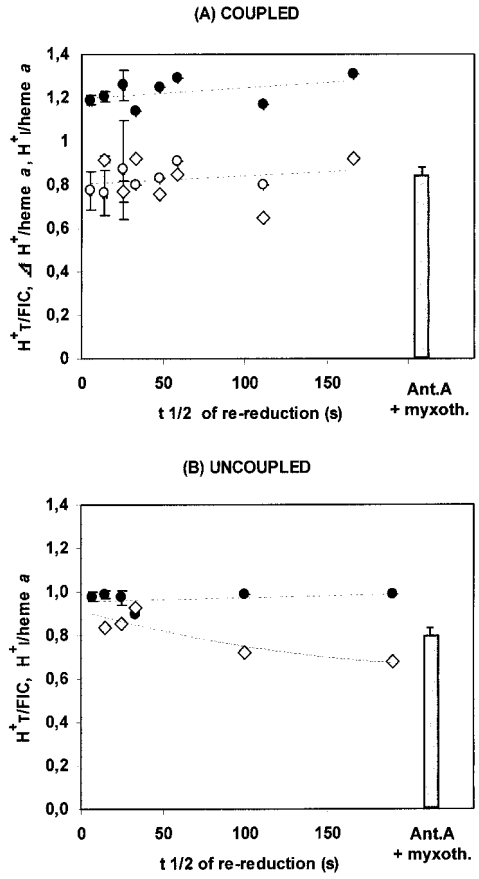

FIGURE 6: Analysis of H^+ transfer linked to redox transitions of the metal centers in CO-liganded cytochrome *c* oxidase vesicles. The experimental conditions are those described in the legend of Figure 4. The rate of rereduction of the metal centers, expressed as $t_{1/2}$, was varied by changing the concentration of malonate. The experiments were performed in the absence (A) and in the presence (B) of 3 μM CCCP: black circles, H^+_T/FIC, i.e., the ratio between the total amount of H^+ released following the oxidation/reduction cycle of heme *a* and the amount of oxidizing equivalents added as ferricyanide; white diamonds, H^+_I/heme *a*, i.e., the ratio between the initial proton release associated with the rapid oxidation of metal centers elicited upon addition of ferricyanide and the amount of oxidized heme *a*; white circles, ΔH^+/heme *a*, i.e., the ratio between the extra H^+ release with respect to the amount of ferricyanide added and the amount of heme *a* undergoing oxido−reduction. The columns indicate the H^+/heme *a* ratio obtained in the presence of antimycin A plus myxothiazol and refer to the overall H^+ release associated with the permanent oxidation of heme *a*. The values are means of at least three different determinations and the bars indicate SEM; the difference between the H^+_T/FIC measured in the coupled and uncoupled conditions is highly statistically significant ($P < 0.0005$).

did not exhibit, for both heme *a* and Cu_A, any detectable deviation from regular Nernstian plots of degree of reduction versus Eh (data not shown). This was, in fact, expected as heme *a* and Cu_A were found to have, in the pH range explored (6.0−8.5), the same Em values (*21*). A second consequence of this interactive H^+/e^- cooperative coupling is that while the one electron reduction of the Cu_A/heme *a* center is sufficient to induce maximal protonation, at the given pH of the coupled acid−base groups, release of the H^+ bound to the fully reduced oxidase will take place only when both heme *a* and Cu_A are oxidized (Figure 7).

The results obtained with the oxidase reconstituted in liposomes show that the proton transfer resulting from the redox Bohr effects linked to heme *a* and Cu_A displays

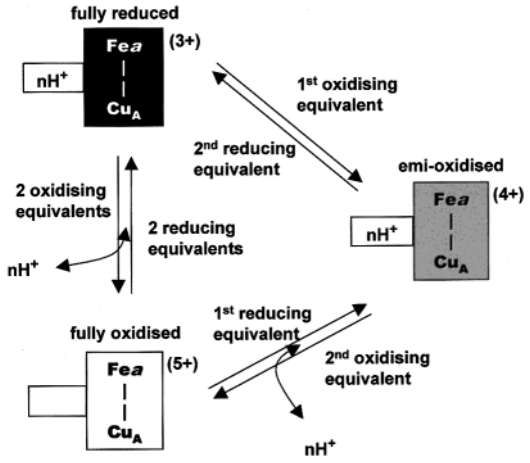

FIGURE 7: Model of interactive proton release/uptake coupled with oxidation/reduction of Cu_A and heme *a* in CO-inhibited cytochrome *c* oxidase.

vectorial asymmetry; i.e., the protons are taken up from the inner space, upon reduction of these centers, and released in the external space, upon their oxidation. This direction of the proton uptake and release is just what is expected from a direct involvement of this cooperative linkage at Cu_A and heme *a* (redox Bohr effect) in the proton pump of the oxidase. Other experiments have provided evidence showing that also in the unliganded cytochrome *c* oxidase the redox Bohr effect coupled to heme *a* and Cu_A displays the same vectorial asymmetry (*35*).

It should be recalled that the proton release in the external phase and the proton uptake from the inner space, coupled to oxidation and reduction of heme *a* and Cu_A, respectively, represent reactions each associated with half-turnover of these centers. It is conceivable that in the turning over unliganded oxidase in the membrane in the respiring steady state, upon transfer of each electron by Cu_A and heme a in sequence, from cytochrome *c* to the binuclear heme a_3-Cu_B center, up to about 1 H^+ will be taken up from the inner aqueous space and translocated to the outer phase, directly or after transient trapping by acid−base group(s), whose p*K*s are linked to the chemistry of oxygen reduction to H_2O at the binuclear heme a_3-Cu_B center. The latter reaction plays, in fact, a primary role in the energy-yelding process and possibly in the step of H^+ release in the outer aqueous phase (*36*−*38*). Work is in progress in our laboratory to identify the chemical nature of the acid−base groups, whose p*K*s are linked to oxido−reduction of heme *a* and Cu_A. The crystallographic data available show possible proton input pathways leading from the inner aqueous space to regions close to heme *a* (*39*, *40*). Different pathways for proton release from the environment of the redox centers of the oxidase into the outer aqueous phase have, on the other hand, been proposed (*36*, *40*).

ACKNOWLEDGMENT

This work was financially supported by grants from the National Project on Bioenergetics and Biomembranes 1999 of the Italian Ministry for the University and Scientific and Technological Research (MURST) and the Finalised Project for Biotechnology of the Italian Research Council (CNR, Rome), Project No. 99.03622.PF49.

REFERENCES

1. Mitchell, P., and Moyle, J. (1970) In *Electron Transport and Energy Conservation* (Tager, J. M., and et al., Eds), pp 575−587, Adriatica Editrice, Bari, Italy.
2. Papa, S. (1976) *Biochim. Biophys. Acta 456*, 39−84.
3. Wikstrom, M., Krab, K., and Saraste, M. (1981) *Cytochrome c oxidase. A Synthesis*, pp 11−115, Academic Press, London.
4. Ferguson-Miller, S., and Babcock, G. T. (1996) *Chem. Rev. 96*, 2889−2907.
5. Gelles, J., and Chan, S. I. (1985) *Biochemistry 24*, 3963−3972.
6. Chan, S. I., and Li, P. M. (1990) *Biochemistry 29*, 1−12.
7. Artzatbanov, V. Y., Konstantinov, A. A., and Skulachev, V. P. (1978) *FEBS Lett. 87*, 180−185.
8. Wikstrom, M. (1981) In *Chemiosmotic Proton Circuits in Biological Membranes* (Skulachev, V. P., and Hinkle, P. C., Eds), pp 171−180.
9. Babcock, G. T., and Callahan, P. M. (1983) *Biochemistry 22*, 2314−2319.
10. Rousseau, D. L., Sassaroli, M., Ching, Y. C., and Dasgupta, S. (1988) *Ann. N.Y. Acad. Sci. 550*, 223−237.
11. Papa, S., Capitanio, N., and Villani, S. (1998) *FEBS Lett. 439*, 1−8.
12. Wikstrom, M., Bogachev, A., Finel, M., Morgan, J. E., Puustinen, A., Raitio, M., Verkhovskaya, M., and Verkhovsky, M. I. (1994) *Biochim. Biophys. Acta 1187*, 106−111.
13. Iwata, S., Ostermeier, C., Ludwig, B., and Michel, H. (1995) *Nature 376*, 660−669.
14. Clark, W. M. (1960) *Oxidation−Reduction Potentials of Organic Systems*, The Williams and Wilkins Company, Baltimore, MD.
15. Papa, S., Guerrieri, F., Lorusso, M., and Simone, S. (1973) *Biochimie 55*, 703−716.
16. Wyman, J. (1968) *Annu. Rev. Biophys. Biophys. Chem. 1*, 35−80.
17. Dutton, P. S. (1978) *Methods Enzymol. 54*, 411−435.
18. Papa, S., Guerrieri, F., and Izzo, G. (1986) *Methods Enzymol. 126*, 331−343.
19. Capitanio, N., Vygodina, T. V., Capitanio, G., Konstantinov, A. A., Nicholls, P., and Papa, S. (1997) *Biochim. Biophys. Acta 1318*, 255−265.
20. Papa, S., and Capitanio, N. (1998) *J. Bioenerg. Biomembr. 30*, 109−119.
21. Capitanio, N., Capitanio, G., Minuto, M., De Nitto E., Palese, L. L., Nicholls, P., and Papa, S. (2000) *Biochemistry 39*, 6373−6379.
22. Ellis, W. R., Wang, H., Blair, D. F., Gray, H. B., and Chan, S. I (1986) *Biochemistry 25*, 161−167.
23. Wilson, D. F., Erecinska, M., and Owen, C. S. (1976) *Arch. Biochem. Biophys. 175*, 160−177.
24. Van Gelder, B. F., Van Rijin, J. L. M. L., Schilder, G. J. A., and Wilms, J. (1977) in *Structure and Function of Energy-transducing Membranes* (Van Dam, K., and Van Gelder, B. F., Eds), pp 61−68, Elsevier/North-Holland, Amsterdam.
25. Erecinska, M., Chance, B., and Wilson, D. F. (1971) *FEBS Lett. 19*, 284−286.
26. Mitchell, R. (1991) The Nature and Significance of the pH-Dependence of Electron Equilibration in the Cytochrome c oxidase System, Ph.D. Thesis, King's College, London, UK.
27. Verkhovsky, M. I., Belevich, N., Morgan, J. E., and Wikstrom, M. (1999) *Biochim. Biophys. Acta 40384*, 1−6.
28. Errede, B., Kamen, M. O., and Hatefi, Y. (1978) *Methods Enzymol. 53*, 40−47.
29. Kadenbach, B., Jaraush, J., Hartman, R., and Merle, P. (1983) *Anal. Biochem. 120*, 517−521.
30. Casey, R. P., Chappel, J. B., and Azzi, A. (1979) *Biochem. J. 182*, 149−156.
31. Papa, S., Capitanio, N., and De Nitto, E. (1987) *Eur. J. Biochem. 164*, 507−516.
32. Casey, R. P., Ariano, B. H., and Azzi, A. (1981) *Eur. J. Biochem. 122*, 313−318.
33. Nicholls P. (1978) *Biochem. J. 175*, 1147−1150.

34. Wrigglesworth, J. M., Eldsen, J., Chapman, A., Van der Water, N., and Grahm, M. F. (1988) *Biochim. Biophys. Acta 936*, 452−464.
35. Capitanio, N., Capitanio, G., De Nitto, E., and Papa, S. (1997) *FEBS Lett. 414*, 414−418.
36. Michel, H. (1998) *Proc. Natl. Acad. Sci. U.S.A. 95*, 12819−12824.
37. Rich, P. R. (1995) *Aust. J. Plant Physiol. 22*, 479−486.
38. Michel, H. (1999) *Biochemistry 38*, 15129−15140.
39. Tsukihara, T., Asyama, H., Yamashita, E., Tomizaki, T., Yamagushi, H., Shinzawa-Itoh, K., Nakashima, R., Yaono, R., and Yoshikawa, S. (1996) *Science (Tokoyo) 272*, 1136−1144.
40. Yoshikawa, S., Shinzawa-Itoh, K., Nakashima, R., Yaono, R., Yamashita, E., Inoue, N., Yao, M., Jei Fei, M., Libeu, C. P., Mizushima, T., Yamagushi, H., Tomizaki, T., and Tsukihara, T. (1998) *Science (Tokoyo) 280*, 1723−1729.

BI001940Z